EUROPEAN ORGANIZATION FOR NUCLEAR RESEARCH
CERN – ACCELERATORS AND TECHNOLOGY SECTOR

CERN-ATS-2013-026

# Transformation Heat Treatment of Rapidly Quenched $Nb_3A1$ Precursor Monitored *in situ* by High Energy Synchrotron Diffraction

C. Scheuerlein, A. Ballarino, M. Di Michiel, X. Jin, T. Takeuchi, A. Kikuchi, K. Tsuchiya, K. Nakagawa, T. Nakamoto

**Abstract**

Nb3Al superconductors are studied for use in high field magnets. Fine grained Nb3Al with nearly stoichiometric Al content is obtained by a Rapid Heating Quenching and Transformation (RHQT) process. We describe a non destructive *in situ* study of the transformation process step of a RHQ Nb3Al precursor wire with ramp rates of either 120 °C/h or 800 °C/h. High energy synchrotron x-ray diffraction measurements show the transformation from a Nb(Al)SS supersaturated solid solution into Nb3Al. When heating with a ramp rate of 120 °C/h a strong reduction of the Nb(Al)SS (110) diffraction peak component is observed when the temperature exceeds 660 °C. Additional diffraction peaks are detectable in the approximate temperature interval 610 °C - 750 °C and significant Nb3Al growth is observed above 730 °C.



Presented at ASC 2012
Applied Superconductivity Conference
October 7-12, 2012 – Portland, Oregon, US

Geneva, Switzerland
February 2013

# Transformation heat treatment of rapidly quenched $Nb_3Al$ precursor monitored *in situ* by high energy synchrotron diffraction

C. Scheuerlein, A. Ballarino, M. Di Michiel, X. Jin, T. Takeuchi, A. Kikuchi, K. Tsuchiya, K. Nakagawa, T. Nakamoto

***Abstract*— $Nb_3Al$ superconductors are studied for use in high field magnets. Fine grained $Nb_3Al$ with nearly stoichiometric Al content is obtained by a Rapid Heating Quenching and Transformation (RHQT) process. We describe a non destructive *in situ* study of the transformation process step of a RHQ $Nb_3Al$ precursor wire with ramp rates of either 120 °C/h or 800 °C/h. High energy synchrotron x-ray diffraction measurements show the transformation from a $Nb(Al)_{SS}$ supersaturated solid solution into $Nb_3Al$. When heating with a ramp rate of 120 °C/h a strong reduction of the $Nb(Al)_{SS}$ (110) diffraction peak component is observed when the temperature exceeds 660 °C. Additional diffraction peaks are detectable in the approximate temperature interval 610 °C - 750 °C and significant $Nb_3Al$ growth is observed above 730 °C.**

***Index Terms*— Diffraction, superconducting wires and filaments, $Nb_3Al$.**

## I. INTRODUCTION

THE $Nb_3Al$ phase in superconducting wires for high field magnets [1] is produced during a Rapid Heating Quenching and Transformation (RHQT) process. Unlike the diffusion process, the RHQT process can produce nearly stoichiometric $Nb_3Al$ with small grains [2].

Highest Al content in the $Nb(Al)_{SS}$ solid solution is obtained at roughly 1900 °C [3] and after rapid quenching from this temperature a metastable $Nb(Al)_{SS}$ supersaturated solid solution can be retained. The Rapid Heating and Quenching (RHQ) stages are followed by a transformation heat treatment (HT) at relatively low temperature of typically 800 °C, during which the fine grained A15 phase with high Al content is formed from the $Nb(Al)_{SS}$ solid solution [4].

High energy synchrotron x-ray diffraction is an excellent method for non destructive studies of the phase evolution during the processing of superconducting strands [5]. Here we report an *in situ* study of the $Nb_3Al$ transformation HT by synchrotron x-ray diffraction measurements, which have been performed at the high energy scattering beam line ID15 of the European Synchrotron Radiation Facility (ESRF).

Manuscript received 29 September 2012.

C. Scheuerlein and A. Ballarino are with CERN, CH-1211 Geneva 23, Switzerland, (corresponding author phone: ++41 (0)22 767 8829, e-mail: Christian.Scheuerlein@cern.ch).

M. Di Michiel is with the European Synchrotron Radiation Facility, F-38000 Grenoble, France.

X. Jin, K. Tsuchiya and T. Nakamoto are with High Energy Accelerator Research Organization (KEK), Tsukuba, Ibaraki, 305-0801 Japan.

T. Takeuchi and A. Kikuchi are with National Institute for Materials Science, Tsukuba, Ibaraki, 305-0044 Japan.

K. Nakagawa is with Hitachi Cable Ltd., Tsuchiura, Ibaraki 300-0026, Japan.

## II. EXPERIMENTAL

### *A. The samples*

The $Nb_3Al$ precursor wires (reference K1) were produced by Hitachi Cable, Ltd., using conventional jelly-roll technique. The wires with 222 filaments have a partial interfilamentary Ta matrix. The Ta + Nb matrix to filament volume ratio is 0.8 [1,6]. The RHQ treatment has been performed at the National Institute for Materials Science (NIMS). After the RHQ treatment the wire diameter is reduced from 1.3 mm to 0.7 mm by cold drawing.

Diffraction measurements have been performed on two RHQ $Nb_3Al$ wire samples, one without and one with electrodeposited Cu stabiliser (nominal diameters of the final wire are 0. 7 mm and 1.0 mm, respectively).

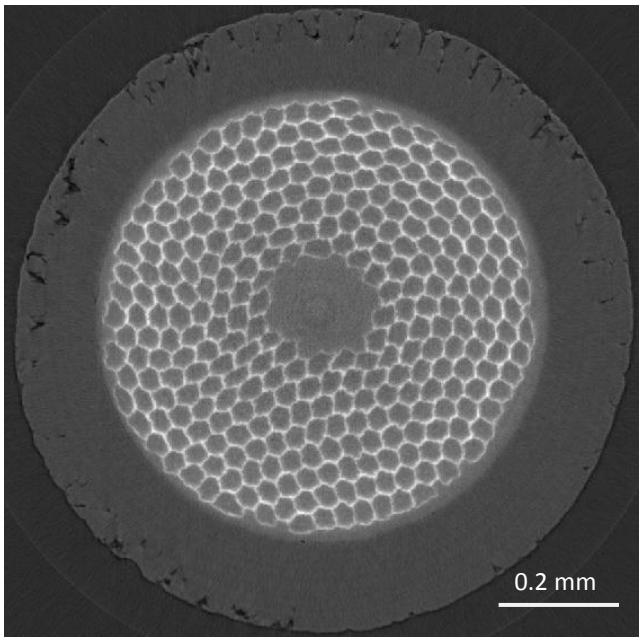


Fig. 1: Tomographic cross section of as-quenched $Nb_3Al$ precursor wire with interfilamentary Ta matrix and electrodeposited Cu stabiliser.

A tomographic cross section of a RHQ $Nb_3Al$ wire obtained by synchrotron tomography is shown in Fig.1. In the tomogram

Nb and Ta can be easily distinguished by the absorption contrast (the strongly absorbing Ta matrix appears brightest).

*B. X-ray powder diffraction*

X-ray powder diffraction measurements were performed at the ID15A beam line of ESRF using a monochromatic 70 keV X-ray beam. Diffraction measurements were performed in transmission geometry and Debye-Scherrer diffraction patterns were acquired with a high-efficiency, high-readout-speed area detector (Trixell Pixium 4700). The beam size was 0.3×0.3 $mm^2$.

The strain free crystallographic parameters at RT of the phases detected in the $Nb_3Al$/Cu wire are summarised in Table 1. Strain free Ta and Nb lattice parameters at RT differ by about 0.03 % only. Therefore, diffraction peaks of both phases overlap, and in the present experiment Nb and Ta cannot be distinguished by their lattice spacing. Unless explicitly mentioned, in the following by Nb peak we refer to both overlapping Nb and Ta peaks.

TABLE 1 Crystallographic parameters of the different phases in the $Nb_3Al$/Cu wire. *The lattice parameter for supersaturated solid solution $Nb(Al)_{SS}$ decreases linearly with increasing Al content. The value reported for $Nb(Al)_{SS}$ with 21.5 at.% Al is 3.276 Å [7]. **The $Nb_3Al$ lattice parameter varies linearly with Al composition from 5.197-5.180 Å in the range 19-25 at.% [7]. The lattice parameter reported for $Nb_3Al$ powder extracted from a fully processed K1 wire is 5.186 Å [8].

| Phase | Space group | Lattice parameter (Å) |
|---|---|---|
| Nb* | Im-3m | 3.3004 |
| Ta | Im-3m | 3.3013 |
| $Nb_3Al$** | Pm-3n | 5.197-5.180 |
| Cu | Fm-3m | 3.615 |

*C. The in situ heat treatment (HT)*

Two different *in situ* heat treatments (HT) were performed in the ID15 resistive tomography-diffraction furnace in $N_2$ inert gas. The furnace temperature has been regulated using a thermocouple spot welded onto the $Nb_3Al$/Cu or $Nb_3Al$ wire sample. The sample temperature accuracy is better than ±2 °C. The ramp rate was either 120 °C/h or 800 °C/h (for comparison, the ramp rate during a transformation HT is typically between 200 and 800 °C/h [4]). Unlike in a standard transformation HT, during the 120 °C/h HT the 800 °C plateau has been omitted, and the maximum temperature was 1100 °C, slightly above the Cu melting temperature of 1085 °C. Diffractograms have been acquired every 5 minutes, i.e. every 10 °C and every 67 °C during the 120 °C/h and 800 °C/h ramp rate, respectively.

## III. Results

*A. Static diffraction results of the RHQ wire before transformation HT*

Fig 2 shows a diffraction image of the $Nb_3Al$/Cu precursor wire after rapid heating and quenching as recorded with the Trixell Pixium 4700 detector. The calibrated two-dimensional diffraction patterns were caked into 128 sectors. Fig 3 shows the sequence of sectorised data. Four diffraction rings (Nb (110), Cu (111), Cu (200) and Nb (200)) are recorded entirely. For Nb (211), Cu (220) and Nb (220) the reflections at crystalline planes oriented perpendicular to the wire drawing direction (sector 1) are not recorded with the rectangular detector. The non homogeneous intensity distribution in the Nb diffraction rings is a sign of the $Nb(Al)_{ss}$ texture in the wire.

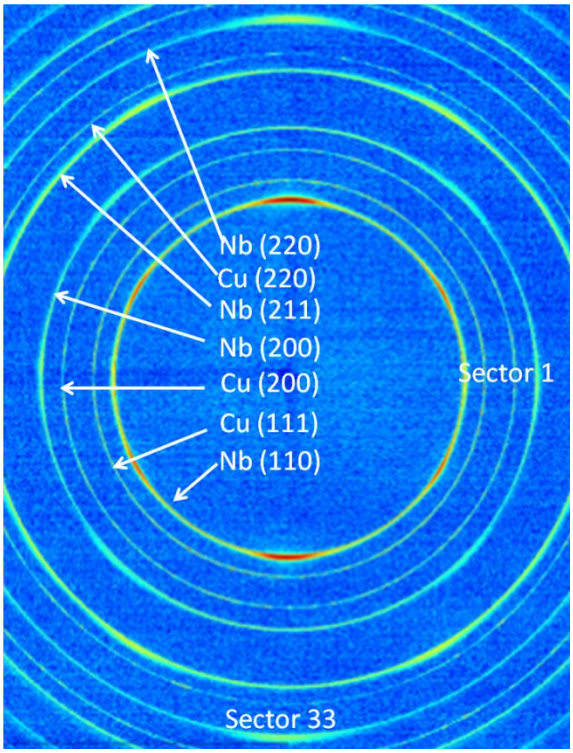


Fig. 2: Diffraction pattern of the as-quenched $Nb_3Al$/Cu wire as recorded with the Trixell Pixium 4700 detector.

The radially integrated diffraction pattern from crystalline planes oriented in the wire drawing direction (axial) and perpendicular to the wire axis (transversal) are shown in Fig. 3. The pattern in the opposing cakes 1 and 65, as well as in 33 and 97 have been summed up in order to improve signal to noise ratio in the diffractograms.

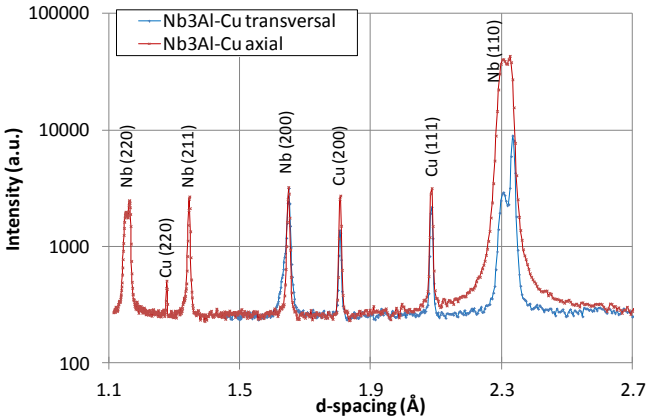


Fig. 3: Radially integrated diffraction pattern of RHQ Nb3Al/Cu wire. Only the sectorised data for crystalline planes in the wire drawing direction (axial) and perpendicular to the wire drawing direction (transversal) are shown.

The Nb (110) and Nb (200) peaks are shown in Fig. 4. The axial and transverse Nb (110) peaks exhibit two maxima, which are characteristic for pure Nb and Ta (larger d-spacing) and

$Nb(Al)_{ss}$ supersaturated solid solution (with roughly 1% smaller d-spacing).

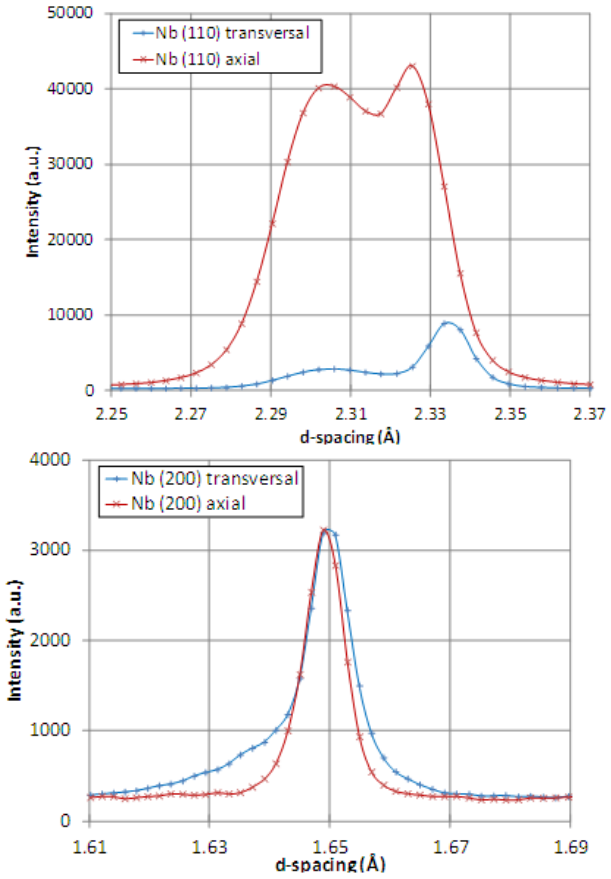


Fig. 4: Radially integrated diffraction pattern of Nb (110), and Nb (220) peaks in transverse (sector 1+65) and axial (sector 33+97) direction.

The Nb (and Ta), $Nb(Al)_{SS}$ and Cu d-spacings are summarized in Table 2, together with the calculated lattice parameters.

TABLE 2 d-spacing of selected diffraction peaks.

| Peak | d-spacing (Å) | Lattice parameter (Å) |
|---|---|---|
| Nb (110)-t | 2.336 | 3.304 |
| $Nb(Al)_{SS}$ (110)-t | 2.306 | 3.261 (-1.3 %) |
| Nb (110)-a | 2.326 | 3.289 |
| $Nb(Al)_{SS}$ (110)-a | 2.304 | 3.258 (-0.94 %) |
| Nb (200)-t | 1.650 | 3.300 |
| Nb (200)-a | 1.648 | 3.296 |
| Nb (220)-a | 1.163 | 3.289 |
| $Nb(Al)_{SS}$ (220)-a | 1.152 | 3.258 (-0.94 %) |
| Nb (211)-a | 1.346 | 3.297 |
| Cu (111)-t | 2.086 | 3.613 |
| Cu (111)-a | 2.086 | 3.613 |
| Cu (220)-a | 1.277 | 3.612 |

The Nb (110)-axial to Nb (110)-transverse integrated peak intensity ratio is 7.6, indicating that some degree of Nb (and/or Ta) texture, which is developed during the cold drawing of bcc metals, is retained during the RHQ process.

As expected, the Cu stabilizer, which is electrodeposited after the wire cold drawing and RHQ process, does not exhibit a strong texture. The measured Cu lattice parameters in axial and transverse direction are identical and correspond with the published strain free lattice parameter.

*B. Transformation HT with 800 °C/h*

A RHQ $Nb_3Al$ wire without Cu stabiliser was heated with a ramp rate of 800 °C/h and a final 800 °C plateau lasting 30 minutes. The evolution of the Nb (110), $Nb_3Al$ (200) and $Nb_3Al$ (211) diffraction peak shape and intensity during this HT is shown in Fig. 5. An obvious variation in the diffractograms is the vanishing of the $Nb(Al)_{SS}$ peak component and the appearance of $Nb_3Al$ peaks.

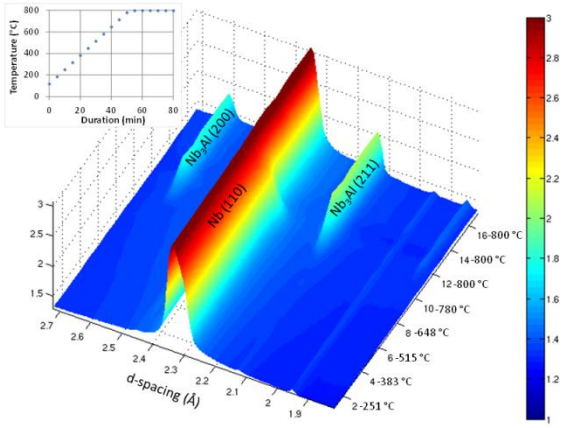


Fig. 5: Evolution of $Nb_3Al$ (200), Nb (110) and $Nb_3Al$ (211) peaks during *in situ* HT of RHQ $Nb_3Al$ wire with a ramp rate of 800 °C/h (see inset). Every 5 minutes a diffractogram was acquired (the temperature is shown on the right axis). Diffractograms No. 12-17 were acquired at 800 °C.

The radially integrated diffractograms acquired during the transformation HT at 581 °C, 648 °C, 714 °C, 780 °C and at 798 °C are presented in Fig. 6.

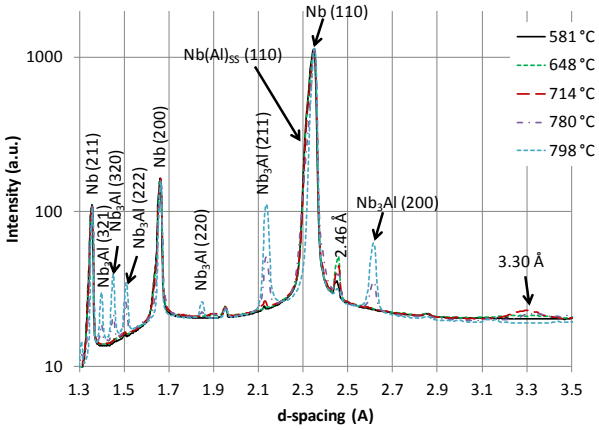


Fig. 6: Diffractograms acquired during *in situ* HT of RHQ $Nb_3Al$ wire in the temperature range 581 °C-798 °C.

Apart from the $Nb_3Al$ peaks, new peaks, whose d-spacing at 800 °C is roughly 2.46 Å and 3.30 Å, are detected in the diffractograms. The not yet identified peak with an

approximate d-spacing of 2.46 Å might be characteristic for an oxide, which formation during the transformation HT has been reported in [9]. The 2.46 Å peak is first detected at about 500 °C and the maximum peak area is obtained at about 650 °C.

The very broad peak with d-spacing of 3.30 Å has been assigned to $Nb(Al)_{SS}$ (100) [10], and is detected between 650 °C and 780 °C.

The integrated peak breadth (defined as the ratio of the peak area to the maximum peak intensity) of the Nb (110) peak decreases simultaneously with the integrated peak intensity when the temperature exceeds 720 °C, due to the disappearance of the overlapping $Nb(Al)_{SS}$ (110) peak component.

The $Nb_3Al$ peaks are first detected in the diffractorgram acquired at 780 °C. During the 30 minutes 800 °C plateau the Nb and $Nb_3Al$ integrated peak intensities do not change strongly.

$Nb_2Al$ is not detected in the diffractograms at any stage of the transformation HT, indicating that when heating with a ramp rate of 800 °C/h the change of the crystallite structure occurs essentially without variations of the elemental wire composition.

### *C. Transformation HT with 120 °C/h to 1100 °C*

A sequence of all diffractograms that have been acquired during the 120 °C/h transformation HT is shown in Fig. 7. When heating with this ramp rate the $Nb(Al)_{SS}$ (110) peak component starts to decrease already at about 660 °C, and $Nb_3Al$ peak growth is first observed when the temperature exceeds 733 °C. The Cu melting is indicated by the vanishing of the Cu peaks in the diffractogram that has been acquired at 1085 °C.

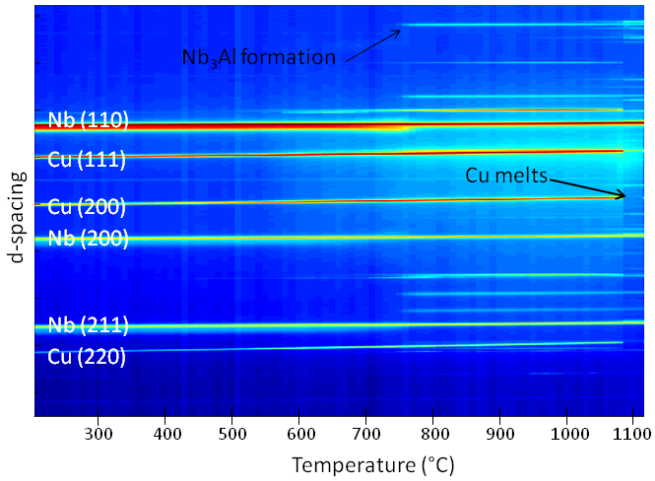


Fig. 7: Colour intensity plot showing the diffraction peak evolution of the rapidly quenched $Nb_3Al$/Cu wire during in-situ HT with 120 °C/h to 1100 °C.

The variation of the Nb (110) diffraction peak during the 120 °C/h HT is presented in Fig. 8. During the 120 °C/h HT the disappearance of the $Nb(Al)_{SS}$ peak component occurs at roughly 60 °C lower temperature as compared to the 800 °C/h HT. Above 773 °C the Nb (110) peak shape and integrated intensity do not change significantly anymore.

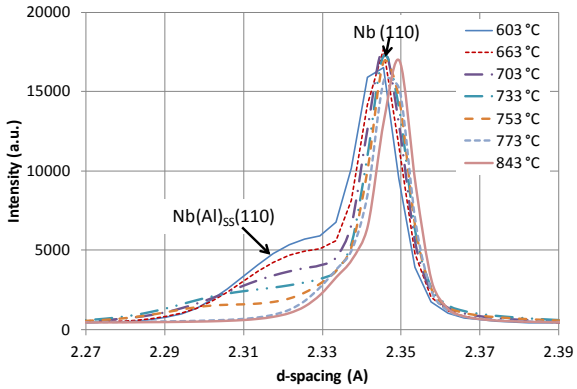


Fig. 8: Nb and $Nb(Al)_{SS}$ (110) diffraction peak evolution during *in situ* HT with a ramp rate of 120 °C/h.

The integrated intensity evolution of selected diffraction peaks is presented in Fig. 9, together with the Nb (110) integrated peak breadth. The decrease of the Nb (110) peak intensity is again accompanied by the growth of a diffraction peak at 3.30 Å ($Nb(Al)_{SS}$ (100)), which is detected in the approximate temperature range 610 °C-750 °C. The onset of $Nb_3Al$ formation is observed at 733 °C, and at 783 °C the nearly maximum amount of $Nb_3Al$ is obtained. The relatively small decrease of the Nb (110) peak area above 800 °C can be explained by thermal lattice motion (Debye–Waller factor).

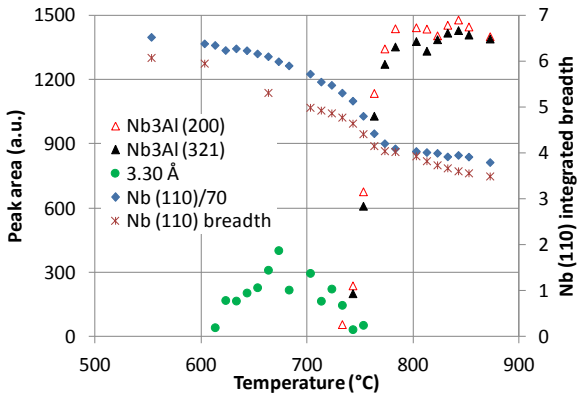


Fig. 9: $Nb_3Al$ (321) and $Nb_3Al$ (320) peak area evolution during transformation HT with 120 °C/h. The Nb (110) peak area was divided by a factor of 70 to fit in the plot.

## IV. Discussion and Conclusion

The transformation of the $Nb(Al)_{SS}$ solid solution, which is retained in the RHQ precursor wire, into $Nb_3Al$ has been monitored *in situ* by high energy synchrotron diffraction measurements during transformation HTs with two different ramp rates (120 °C/h and 800 °C/h).

During the 120 °C/h transformation HT the characteristic changes in the diffractograms that indicate the transformation from a $Nb(Al)_{SS}$ supersaturated solid solution into $Nb_3Al$ occur at roughly 60 °C lower temperature than during the 800 °C/h HT. The different transformation temperature intervals need to be taken into account when performing coil HTs with relatively low ramp rates.

## Acknowledgements

We acknowledge the ESRF for beam time on ID15.

## REFERENCES


[1] T. Nakamoto et al., "R&D Efforts towards High Field Accelerator Magnets at KEK", IEEE Trans. Appl. Supercond., vol. 22, pp. 4003205, 2012

[2] T. Takeuchi, "$Nb_3Al$ Conductors –Rapid Heating, Quenching and Transformation Process-, IEEE. Trans. Supercond., vol. 10(1), pp. 1016-1021, 2000

[3] Niobium(Columbium)-Aluminum," Trans. Met. Soc. AIME, vol. 236, pp. 863-872, 1966

[4] T. Takeuchi, "$Nb_3Al$ Superconductors", IEEE Trans. Appl. Supercond., vol. 12(1), pp. 1088-1093, 2002

[5] C. Scheuerlein, M. Di Michiel, F. Buta, "Synchrotron Radiation Techniques for the Characterization of $Nb_3Sn$ Superconductors", IEEE Trans. Appl. Supercond., vol. 19(3), pp. 2653-2656, 2009

[6] A. Yamamoto, T. Nakamoto, "Magnet Technology Development with $Nb_3Al$ Superconductor for SLHC", presentation at CERN-KEK committee, 29.3.2010, goo.gl/V2IQa

[7] J.L. Jorda, R. Flukiger, J. Muller, "A New Metallurgical Investigation of the Niobium-Aluminum System", Journal of the Less Common Metals vol. 75(2), pp. 227‑239, 1980

[8] X. Jin, T. Nakamoto, T. Ito, S. Harjo, A. Kikuchi, T. Takeuchi, K. Tsuchiya T. Hemmi, T. Ogitsu, A. Yamamoto, "Residual strain dependence on the matrix structure in RHQ-Nb3Al wires by neutron diffraction measurement", Supercond. Sci. Technol. 25, pp. 065021, 2012

[9] A. Kikuchi, Y. Iijima, K. Inoue, "Microstructures and superconducting properties of transformed $Nb_3Al$ wires", Physica C 372–376, pp. 1307–1310, 2002

[10] T Takeuchi, N Banno, T Fukuzaki, H Wada, "Large improvement in high-field critical current densities of $Nb_3Al$ conductors by the transformation-heat-based up-quenching method", Supercond. Sci. Technol. 13(10), pp. L11-L14, 2000